OFFPRINT

A mesoscopic model for the effect of density on pedestrian group dynamics

F. ZANLUNGO and T. KANDA

Please visit the website
www.epljournal.org

The Editorial Board invites you to submit your letters to EPL

EPL is a leading international journal publishing original, innovative Letters in all areas of physics, ranging from condensed matter topics and interdisciplinary research to astrophysics, geophysics, plasma and fusion sciences, including those with application potential.

The high profile of the journal combined with the excellent scientific quality of the articles ensures that EPL is an essential resource for its worldwide audience. EPL offers authors global visibility and a great opportunity to share their work with others across the whole of the physics community.

Run by active scientists, for scientists

EPL is reviewed by scientists for scientists, to serve and support the international scientific community. The Editorial Board is a team of active research scientists with an expert understanding of the needs of both authors and researchers.

A mesoscopic model for the effect of density on pedestrian group dynamics

F. ZANLUNGO and T. KANDA

Intelligent Robotics and Communication Laboratories, ATR - Kyoto, Japan and
Japan Science and Technology Agency, CREST

Abstract – We introduce a mesoscopic model of pedestrian group behaviour, in which the internal group dynamics is modelled using a microscopic potential, while the effect of the environment is modelled using a harmonic term whose intensity depends on a macroscopic quantity, crowd density. We show that, in order to properly describe the behaviour of 2-person groups, the harmonic term is directed orthogonally to the walking direction, and its intensity grows linearly with density. We also show that, once calibrated on 2-person groups, the model correctly predicts the velocity and spatial extension of 3-person groups in the walking direction, while in order to describe properly also the abreast extension of 3-person groups a modification in the microscopic group dynamics has to be introduced. The model also correctly predicts the presence of a bifurcation phenomenon, namely the emergence of a stable 3-person Λ configuration at high densities, while only the V formation is stable at low densities.

Introduction. – Various mathematical methods, often inspired by physical sciences, are used in the study of crowd dynamics [1–9]. A large part of the walking population consists of social groups [10,11], bound systems composed of individual pedestrians which represent for crowds what molecules are in a fluid. Groups walk in a characteristic configuration [10–14] and with slower velocity [11,14–16], and have thus an important influence on the dynamics of the crowd. In the last years a few models describing group dynamics have been introduced [11,17–20]. In our recent works [14,21], we have tried to attain a detailed understanding of the spatial configuration and velocity of groups, both regarding their *free-walking* (or *low-density*, $\rho \to 0$) behaviour and their reaction to growing density conditions.

In [14] we introduced a non-Newtonian[1] potential for the dynamics of socially interacting pedestrian groups *in the low-density limit*[2]. Writing the relative position between 2 socially interacting pedestrians i and j as $\mathbf{r}_{ij} \equiv \mathbf{r}_i - \mathbf{r}_j = (r_{ij}, \theta_{ij})$, where $\theta = 0$ gives the direction to the pedestrians' goal, we made the hypothesis that

the discomfort of i due to not being located in the optimal position for social interaction with j is given by the *microscopic potential*[3]

$$U^{\eta}_{\mathrm{micro}}(r_{ij}, \theta_{ij}) = R(r_{ij}) + \Theta^{\eta}(\theta_{ij}),$$

$$R(r) = C_r \left(\frac{r}{r_0} + \frac{r_0}{r} \right), \tag{1}$$

$$\Theta^{\eta}(\theta) = C_\theta \left((1+\eta)\theta^2 + (1-\eta)(\theta - \mathrm{sign}(\theta)\pi)^2 \right),$$

where r_0 is the most comfortable interaction distance, and $-1 \leq \eta < 0$ is related to the intensity of social interaction. Assuming that the acceleration of the pedestrian i due to group dynamics, *i.e.* to the action of the pedestrian aimed to minimise social interaction discomfort with respect to j, is given by

$$\mathbf{F}_{ij} = -\boldsymbol{\nabla}_i U^{\eta}_{\mathrm{micro}}(\mathbf{r}_{ij}), \tag{2}$$

the radial potential R assures that the pedestrians will have a distance close to r_0, while the angular potential

---

[1]*I.e.*, not obeying the third law of dynamics, see also [22].
[2]The model describes 2- and 3-person group behaviour, but these are found to be the only stable components of larger groups [13,23].

[3]In eq. (1), we are assuming θ to take values in $(-\pi, \pi)$, and using $\mathrm{sign}(0) = -1$ in order to have a continuous potential. Refer to the original work [14] for details.

Θ^η allows them to keep both their interaction partner and their walking goal in sight[4]. The model leads to a Langevin equation for the relative distance $\mathbf{r}$

$$\dot{\mathbf{v}} = -\frac{\mathbf{v}}{\tau} - 2\boldsymbol{\nabla}U_{\mathrm{micro}}^{\eta=0}(\mathbf{r}) + \boldsymbol{\Xi}, \tag{3}$$

where τ is the time scale introduced in [5], and $\boldsymbol{\Xi}$ a Gaussian white noise, and predicts that

– *2-person groups are slower than individual pedestrians, i.e.* naming $v^{(n_g)}$ the average velocity of a group of size n_g, we have

$$v^{(1)} > v^{(2)}; \tag{4}$$

– *3-person groups are even slower, i.e.*

$$v^{(2)} > v^{(3)}, \tag{5}$$

with the following relation holding between the different group velocities:

$$v^{(1)} - v^{(2)} \approx 3(v^{(2)} - v^{(3)}); \tag{6}$$

– *while 2-person groups walk abreast, 3-person groups walk in a V formation*, with the central pedestrian walking slightly behind.

Such predictions resulted to be in very good agreement with the behaviour of pedestrians in a large, straight corridor at low density [14].

In [21], we performed a detailed empirical study regarding the change in shape, spatial extension and velocity of pedestrian groups with density ρ. Regarding group velocities we found that the relations of eqs. (4), (5) are valid for all densities, but the difference between these velocities decreases with growing ρ. Furthermore, the ratio in eq. (6) appears to grow with ρ. Regarding the group shape and extension, we found that the abreast extension of 2- and 3-person groups decreases linearly with ρ, while the average extension in the walking direction of 2- and 3-person groups is independent of ρ. In the case of 2-person groups such an average extension results to be 0, since 2-person groups assume an abreast configuration for all ρ. In the case of 3-person groups, we have a value different from 0, due to a non-abreast configuration that results to be mainly a V formation, with the central pedestrian on the back, for low ρ, but may also be a Λ one, with the central pedestrian on the front, at high densities. The appearance of the Λ configuration at high ρ is counterbalanced by the fact that at high density the V formation is more accentuated (the central pedestrian is more on the back), and thus the average extension in the walking direction does not change in a significant way.

While in [21] we limited ourselves to present our empirical results, in this work we want to show that eq. (1) may be modified introducing a ρ-dependent term that explains how the group dynamics is modified by density. We call this model *mesoscopic*, since it combines the purely microscopic description of eq. (1) with a macroscopic quantity, ρ. While eventually, in order to perform realistic crowd simulations, we want to develop a fully microscopic model of the interaction of groups with the surrounding environment, the details of such a model may be very complex. Due to the extremely simple relation between the group dynamics and the single macroscopic parameter ρ reported in [21], the development of a mathematical model explaining this relation may provide a useful insight and guide the subsequent development of a fully microscopic model. As a first step in this direction, we use in this work the insight obtained comparing the proposed mathematical model with the empirical data in order to improve the description of the 3-person dynamics by introducing a second-neighbour interaction (*i.e.*, between pedestrians on the wings). Furthermore, we use the model to predict the group configuration under high-density conditions.

The model. – The proposed model is extremely simple. Let us consider a group composed of n_g pedestrians, the position of each of them being given, in an arbitrary frame, by $\mathbf{x}_i$. Let us define the group centre position as

$$\mathbf{X} \equiv \frac{\sum_{i=1}^{n_g} \mathbf{x}_i}{n_g}, \tag{7}$$

and the relative distance of i to the centre as

$$\mathbf{r}_i \equiv \mathbf{x}_i - \mathbf{X}. \tag{8}$$

Following eq. (1), we consider each pedestrian in the group to have a common goal given by the unit vector $\hat{\mathbf{g}}$, and for each i we define the clockwise angle θ_i between $\hat{\mathbf{g}}$ and $\mathbf{r}_i$. For each pedestrian, the projection of the position with respect to the centre on the goal direction (direction of walking)[5] is

$$y_i \equiv r_i \cos\theta_i, \tag{9}$$

while the position in the abreast direction is

$$x_i \equiv r_i \sin\theta_i. \tag{10}$$

We will assume that the effect of crowd density manifests itself as a linear recall force with components

$$F_i^x = -K^x(\rho)\frac{x_i}{r_0^2}, \tag{11}$$

$$F_i^y = -K^y(\rho)\frac{y_i}{r_0^2}. \tag{12}$$

Here K^x and K^y are two functions of the macroscopic variable ρ, subject to the conditions

$$K^x(\rho) \geq 0, \qquad K^y(\rho) \geq 0. \tag{13}$$

---

[4]The more negative η is, the more pedestrians will try to have interaction partners in their vision field.

[5]When comparing to empirical data, the direction of walking is defined using the current group velocity.

For a 2-person group, this force may be expressed by adding to the potential of eq. (1) a term[6]

$$U_{\text{macro}}(r, \theta) \equiv \frac{1}{4}\left(K^x(\rho)\frac{r^2 \sin^2 \theta}{r_0^2} + K^y(\rho)\frac{r^2 \cos^2 \theta}{r_0^2}\right).$$

(14)

Model calibration. –

Calibration method. In [14], to which the reader should refer for further details, we introduced a method to calibrate the parameters of eq. (1) by comparing the 2D probability distribution for the pedestrian position in a 2-person group with a Boltzmann distribution

$$\exp(-U(x, y)/T),$$

(15)

where the "temperature" T is determined by the noise in the system due to the environment, *i.e.* by the stochastic term of eq. (3). In this work we are going to apply the same procedure on the data of [21] using a potential given by the sum of eqs. (1) and (10),

$$U_{\text{meso}} \equiv U_{\text{micro}} + U_{\text{macro}}$$

(16)

and, by keeping parameters r_0, C_r and C_θ fixed to their $\rho \to 0$ limit, we are going to determine the functional dependence of $K^x(\rho)$ and $K^y(\rho)$.

Data set. In this work we use the data set introduced in [21] (to which the reader should refer for details[7]), corresponding to 24 hours of automatic pedestrian tracking [24] and video recording in a 3–4 m wide, $\approx 40\,\text{m}$ long passage connecting two busy areas of the ATC multi-purpose centre in Osaka, Japan. The data were collected during different times of the week and the day, in order to observe different density patterns, and the videos were analysed by a human coder in order to identify socially interacting pedestrian groups.

$\rho \to 0$ limit. We assume that the change in the spatial probability distribution of 2-person groups due to density is entirely due to the "macroscopic" term U_{macro} of eq. (14), and thus that r_0 and C_r/C_θ are fixed to their $\rho \to 0$ values, which are obtained in [21] as $r_0 = 0.67\,\text{m}$ and $C_r/C_\theta = 7.5$ (see footnote [8]). The explicit value of C_r does not affect the 2-person distribution, but since

---

[6]The normalisation has been chosen in order to have for K the same dimensionality of C_r, C_θ in eq. (1), while the factor 2 is due to the fact that the distance between the pedestrians in a 2-person group is twice their distance to the group centre.

[7]In particular regarding our definition of density. Note that while in [21] we divided our data in density slots of width $\Delta\rho = 0.01\,\text{ped/m}^2$ when studying the observable averages, and of width $\Delta\rho = 0.05\,\text{ped/m}^2$ when studying the probability distribution functional form, here we use a single slot width of $\Delta\rho = 0.025\,\text{ped/m}^2$.

[8]These values were obtained by calibrating on all the $\rho < 0.05\,\text{ped/m}^2$ data. A different approach would be to use as $\rho \to 0$ limit the values obtained in the large environment of [14], and to introduce a potential term to describe the effect of the narrow environment. This approach leads to results similar to those described here, but the presence of an extra term makes the discussion less clear.
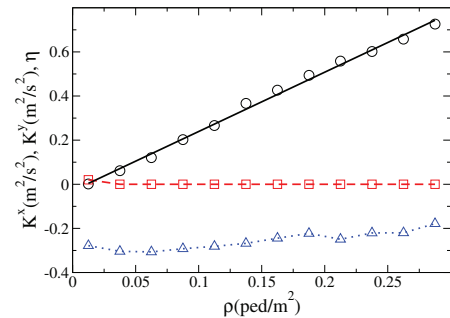

Fig. 1: (Colour on-line) ρ-dependence of K^y, K^x and η. Black circles: K^x, linear best fit in continuous black line. Red squares and dashed line: K^y. Blue triangles and dotted line: ρ-dependence of η that gives the best fit of 2-person group velocities.
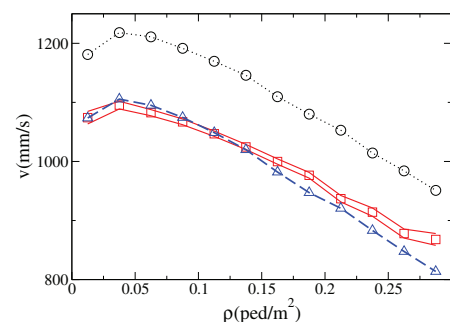

Fig. 2: (Colour on-line) Black circles and dotted line: empirical average value of $v^{(1)}$. Red squares (confidence interval in continuous lines): empirical average value of $v^{(2)}$. Dashed blue line and triangles: average value of $v^{(2)}$ obtained by a numerical integration of the 2-person group system using for each ρ the value of η that provides the best agreement with the empirical velocity in the $\rho \to 0$ limit.

it affects the group velocity and the 3-person distribution, we keep it fixed to the $\rho \to 0$ value obtained in [14] by calibrating on 2- and 3-person group distributions as $C_r = 0.62\,\text{m}^2/\text{s}^2$.

Results. Figure 1 shows the ρ-dependence of K^x, K^y. We may see that we have, for any value of ρ, $K^y \approx 0$, while K^x is described very well (determination coefficient $R^2 = 0.996$) by a linear law $K^x = \alpha + \beta\rho$, with $\beta = 2.689\,\text{m}^4\,\text{ped}^{-1}\,\text{s}^{-2}$ and $\alpha = -0.03\,\text{m}^2/\text{s}^2$ (*i.e.*, negligible with respect to the considered density scale). We thus find that the influence of density grows linearly in the abreast direction, while it is not present in the walking direction.

The parameter η weakly affects the pedestrian position probability distribution, but it has an important effect on the difference between the velocity of individuals and 2-person groups, $v^{(1)} - v^{(2)}$ [14]. By numerically solving[9] the 2-person Langevin equation (3) with the addition of the ρ-dependent term, eq. (14), we find, as reported in fig. 2, that, if we use for all densities the $\rho \to 0$ limit of η

---

[9]With an Euler-Maruyama method, that gives equivalent results using integration steps $\Delta t = 0.1\,\text{s}$ and $\Delta t = 0.025\,\text{s}$.
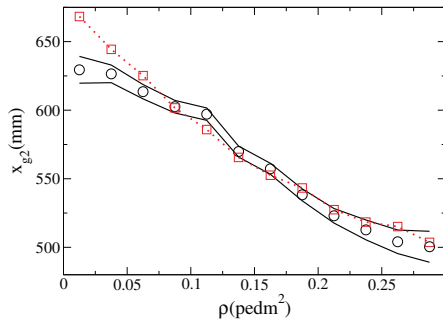
Fig. 3: (Colour on-line) ρ-dependence of x_{g2}. Black circles (confidence intervals in continuous line): empirical average. Dotted red line and squares: average value of x_{g2} in a numerical integration of a 2-person group whose deterministic dynamics is determined by the potential given by eq. (16).

(see footnote [10]), we have a tendency to underestimate the 2-person velocity at high densities. We may thus, by using the approach described in [14], find for each value of ρ the intensity of the stochastic term in the Langevin equation *and* the value of η that provide the best fit to both the position probability distribution and the group velocity. Proceeding in this way, we find for η the ρ-dependence shown in fig. 1, which provides a complete agreement of the model's 2-person velocity with the empirical data. $|\eta|$ appears to decrease with ρ, suggesting, according to the interpretation of η provided in [14], that social interaction decreases at higher density[11].

As discussed in [21], the main effect of ρ on the 2-person spatial configuration is on its abreast extension,

$$x_{g2} \equiv x_2 - x_1, \tag{17}$$

where the pedestrian label is chosen in such a way to have $x_{g2} > 0$. A comparison between the x_{g2} observable in the calibrated system and the corresponding empirical data averages is performed in fig. 3, showing a difference of few cm and comparable to the data precision.

Model evaluation on 3-person groups. – According to [21] the effect of ρ on 3-person groups may be studied using as observables the group velocity $v^{(3)}$, the group abreast extension

$$x_{g3} \equiv x_3 - x_1, \tag{18}$$

and the extension in the walking direction

$$y_{g3} \equiv (y_3 + y_1)/2 - y_2, \tag{19}$$

where, as above, labels are chosen in such a way to have $x_j > x_i$ if $j > i$ (see footnote [12]). We numerically integrate the 3-person system using the "first-neighbour

---

[10]*I.e.*, the one that better describes velocity at low densities.

[11]The dependence of the microscopic parameter η on the macroscopic pedestrian density will thus have to be properly assessed when developing a fully microscopic model.

[12]y_{g3} is defined in order to study the extension of V and Λ formations, refer to [14,21] for details.

Fig. 4: (Colour on-line) ρ-dependence of $v^{(3)}$. Red squares (confidence intervals in continuous line): empirical average. Dashed orange line and triangles: model prediction in the absence of second-order interactions. Dash–double-dotted blue line and asterisks: model prediction using the second-order interaction of eq. (20). Dotted black line and circles show the empirical $v^{(2)}(\rho)$.

Fig. 5: (Colour on-line) ρ-dependence of y_{g3}. Red squares (confidence intervals in continuous line): empirical average. Dashed orange line and triangles: model prediction in the absence of second-order interactions. Dash–double-dotted blue line and asterisks: model prediction using the second-order interaction of eq. (20).
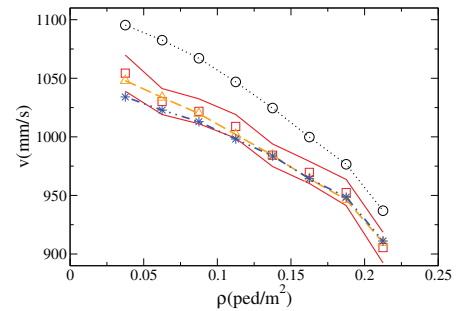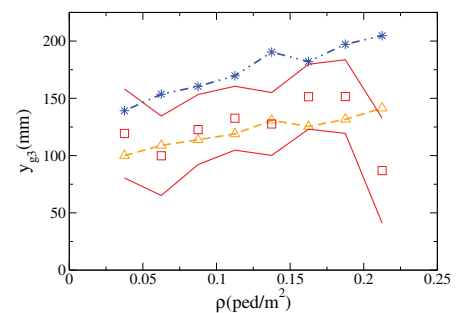

Fig. 6: (Colour on-line) ρ-dependence of x_{g3}. Red squares (confidence intervals in continuous line): empirical average. Dashed orange line and triangles: model prediction in the absence of second-order interactions. Dash–double-dotted blue line and asterisks: model prediction using the second-order interaction of eq. (20).

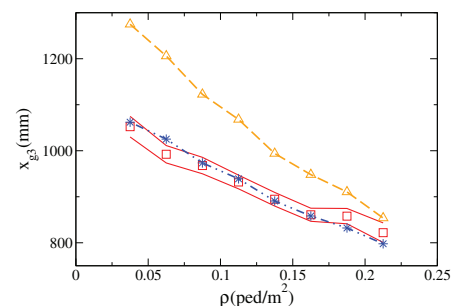interaction" approach described in [14], and compare the empirical and predicted ρ-dependence for these observables in figs. 4, 5 and 6.

We may see that the model predicts very well the ρ-dependence of $v^{(3)}$ and y_{g3}, and in particular the

convergence of $v^{(2)}$ and $v^{(3)}$ at high densities, and the stability of y_{g3} around a positive value (prevalence of V configuration). The ρ-dependence of x_{g3} is, nevertheless, not properly described, and in particular the model strongly under-estimates the 3-person group extension in the low-ρ regime. This problem was already present in [14], where we suggested that the model could be improved by introducing a weaker interaction term between the two pedestrians on the wings (second-neighbour or second-order interaction).

Second-order interaction. We introduce such an interaction taking advantage of the insight obtained from the ρ-dependence model. In order to avoid the introduction of another dimensional parameter, we use for the force between pedestrians 1 and 3 the same radial dependence of the one generated by the potential R in eq. (1), which is

$$\mathbf{F}^{\text{second}} = \alpha \frac{C_r}{r_0} \left(\frac{r_0^2}{r^2} - 1 \right) \frac{\mathbf{r}}{r}, \qquad (20)$$

where $\mathbf{r}$ is the distance between pedestrians 1 and 3, while α determines the relative strength of the second-order interaction with respect to the first-order one. We found that $\alpha = 0.558$ minimises the sum

$$\varepsilon = \varepsilon_{v^{(3)}} + \varepsilon_{y_{g3}} + \varepsilon_{x_{g3}} \qquad (21)$$

of the errors between the numerical and empirical ρ-dependence of $v^{(3)}$, y_{g3} and x_{g3}, which we defined (for example in the $v^{(3)}$ case) as

$$\varepsilon_{v^{(3)}} = \sqrt{\sum_i \left(\frac{v_{\text{num}}^{(3)}(\rho_i) - v_{\text{emp}}^{(3)}(\rho_i)}{\sigma_{v^{(3)}}(\rho_i)} \right)^2}, \qquad (22)$$

where the sum runs over the density slots for which empirical data are available, and σ stands for the data point standard error. As shown in figs. 4, 5 and 6, the second-order interaction strongly increases the ability of the model to describe the abreast extension of 3-pedestrian groups, while preserving a correct description of velocity and extension in the direction of motion. Furthermore, the introduction of an interaction between all pedestrians makes the model numerically stable also at high values of ρ, and allows us to investigate the model's prediction for group configuration and velocity at high density. A term similar to eq. (20) should thus be introduced also when developing a fully microscopic model of 3-person groups.

Model predictions. –

High-density behaviour. We study the prediction of the model regarding densities up to one order of magnitude higher than those available in the data set. For simplicity, we fix η to its $\rho \to 0$ value, and, although $v^{(1)}$, and, as a consequence $v^{(2)}$ and $v^{(3)}$, are decreasing functions of ρ (figs. 2, 4), we assume $v^{(1)} = 1\,\text{m/s}$ for all ρ. We then study how the main group observables vary with $K^x = \beta\rho$, where β is given by the best fit of fig. 1. As shown in
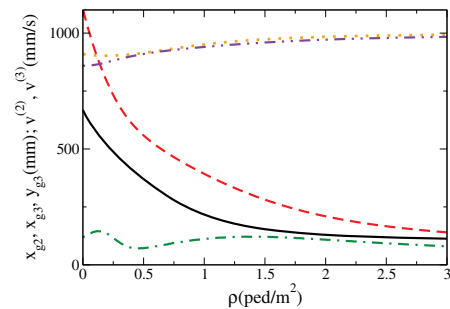

Fig. 7: (Colour on-line) Predicted ρ-dependence of: x_{g2} (continuous black line); x_{g3} (dashed red line); y_{g3} (dash-dotted green line); $v^{(2)}$ (dotted orange line); $v^{(3)}$ (dash–double-dotted magenta line).
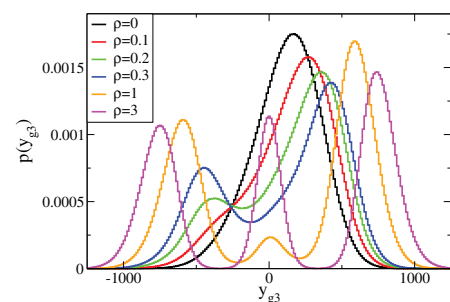

Fig. 8: (Colour on-line) y_{g3} probability distribution at different ρ values.

fig. 7, since $v^{(3)}$ initially grows faster than $v^{(2)}$, the 2- and 3-person group velocities assume basically the same value at $\rho \approx 0.5\,\text{ped/m}^2$, and then gradually converge to $v^{(1)}$. y_{g3} has a non-trivial dynamics, but its value is always positive and its variation limited to the 70–150 mm range. For the x_{g2} and x_{g3} variables, the model shows that the linear decrease law cannot be extrapolated beyond the empirically observed range. Furthermore, at densities larger than $1\,\text{ped/m}^2$, 2- and 3-person groups show x extensions of the order of 100–200 mm, clearly not compatible with abreast or V configurations. These results suggest that at high density pedestrians start walking in a line.

V-Λ and abreast-line bifurcations. In [21] we reported a transition in the 3-person group configuration: with growing density, along the V formation also a Λ configuration with the central pedestrian walking on the front becomes stable. This transition manifests itself as the emergence of a local maximum for negative y in the y_{g3} distribution. Figure 8 shows the y_{g3} distribution, as numerically predicted by our model, for a few values of ρ. While at $\rho = 0$ a single maximum is present at $y > 0$, at higher densities a second, $y < 0$ maximum emerges (Λ configuration). At even higher densities the two maxima assume positions farther from 0, and then a third maximum, that eventually stabilises at $y = 0$, emerges. The line configuration corresponds to the situation in which 3 almost equal maxima are present (the "central" pedestrian may now be in the front, middle or back position of the line).
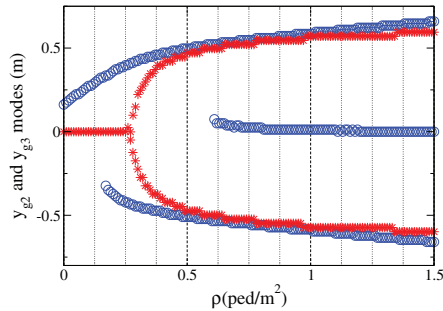
Fig. 9: (Colour on-line) Red asterisks: position of the y_{g2} distribution maxima as a function of ρ. Blue circles: position of the y_{g3} distribution maxima as a function of ρ.

An "abreast-line" bifurcation is present also in 2-person systems. Figure 9 shows the ρ-dependence of the position of the maxima in the probability distribution of y_{g3} and $y_{g2} \equiv y_2 - y_1$. It may be seen that at the critical density $\rho \approx 0.26 \, \text{ped/m}^2$ we have a bifurcation in the y_{g2} distribution, and pedestrians gradually abandon the abreast configuration and start following each other. As described above, for the 3-person group we have two different bifurcation phenomena, one happening at $\rho \approx 0.17 \, \text{ped/m}^2$, and corresponding to the appearance of a stable Λ formation, and a second one at $\rho \approx 0.6 \, \text{ped/m}^2$, the density at which the left-right symmetry of V and Λ formations is broken and pedestrians gradually start walking in a line.

These predictions of the model could be tested by comparing to new high-density data, when these data will be available. It has nevertheless to be stressed that the model describes pedestrians having social interactions regardless of the high-density conditions. As soon as pedestrians stop interacting, we can put $C_\theta \approx 0$ in eq. (1) and walking in a line and Λ formations become possible even at low densities, as observed in [21]. It may indeed be mathematically shown that for a 2-person group with $C_\theta = 0$ walking in a line is a stable configuration for any $\rho > 0$; the switching behaviour described in [18] may thus be obtained in our model by temporarily putting the value of C_θ to 0.

Conclusions. – We have introduced a mesoscopic model of pedestrian group behaviour, in which the internal group dynamics is modelled using a microscopic potential, while the effect of the environment is modelled using a harmonic term whose intensity depends on the macroscopic crowd density. We showed that, in order to properly describe the behaviour of 2-person groups, the harmonic term is directed orthogonally to the walking direction, and its intensity grows linearly with density. We also showed that the model calibrated on 2-person groups correctly predicts the velocity and spatial extension of 3-person groups in the walking direction. In order to describe properly also the abreast extension of 3-person groups we introduced a modification in the microscopic model, and namely an interaction term between the two

pedestrians on the wings. The model also correctly predicts the emergence of a stable 3-person Λ configuration at high densities, while only the V formation is stable at low densities. Another bifurcation phenomenon, switching to walk in a line, is also predicted to occur at higher densities, both for 2- and 3-person groups.

REFERENCES

[1] HENDERSON L., *Nature*, **229** (1971) 381.
[2] KACHROO P. P., AL-NASUR S. J. and WADOO S. A., *Pedestrian Dynamics: Feedback Control of Crowd Evacuation* (Springer) 2008.
[3] MURAMATSU M. and NAGATANI T., *Physica A: Stat. Mech. Appl.*, **286** (2000) 377.
[4] BURSTEDDE C., KLAUCK K., SCHADSCHNEIDER A. and ZITTARTZ J., *Physica A: Stat. Mech. Appl.*, **295** (2001) 507.
[5] HELBING D. and MOLNAR P., *Phys. Rev. E*, **51** (1995) 4282.
[6] HOOGENDOORN S. and DAAMEN W., in *Traffic and Granular Flow '03* (Springer) 2005, p. 373.
[7] KRETZ T., GRÜNEBOHM A., KAUFMAN M., MAZUR F. and SCHRECKENBERG M., *J. Stat. Mech.: Theory Exp.* (2006) P10001.
[8] KARAMOUZAS I., SKINNER B. and GUY S. J., *Phys. Rev. Lett.*, **113** (2014) 238701.
[9] HELBING D. and JOHANSSON A., *Encycl. Complex. Syst. Sci.*, **16** (2009) 6476.
[10] SCHULTZ M., RÖSSGER L., FRICKE H. and SCHLAG B., in *Pedestrian and Evacuation Dynamics 2012* (Springer) 2014, pp. 1097–1111.
[11] MOUSSAÏD M., PEROZO N., GARNIER S., HELBING D. and THERAULAZ G., *PLoS ONE*, **5** (2010) e10047.
[12] COSTA M., *J. Nonverbal Behav.*, **34** (2010) 15.
[13] ZANLUNGO F. and KANDA T., presented at *COGSCI13*, 2013.
[14] ZANLUNGO F., IKEDA T. and KANDA T., *Phys. Rev. E*, **89** (2014) 012811.
[15] KLÜPFEL H., in *Pedestrian and Evacuation Dynamics 2005* (Springer) 2007, pp. 285–296.
[16] SCHULTZ M., SCHULZ C. and FRICKE H., in *Pedestrian and Evacuation Dynamics 2008* (Springer) 2010, pp. 381–396.
[17] KÖSTER G., SEITZ M., TREML F., HARTMANN D. and KLEIN W., *Contemp. Soc. Sci.*, **6** (2011) 397.
[18] KARAMOUZAS I. and OVERMARS M., in *Proceedings of 17th ACM Symposium VRST* (ACM) 2010, pp. 183–190.
[19] ZHANG Y., PETTRÉ J., QIN X., DONIKIAN S. and PENG Q., in *Proceedings of CAD/Graphics 2011* (IEEE) 2011, pp. 275–281.
[20] CHENG L., YARLAGADDA R., FOOKES C. and YARLAGADDA P. K., *World*, **1** (2014) 002.
[21] ZANLUNGO F., BRŠČIĆ D. and KANDA T., *Phys. Rev. E*, **91** (2015) 062810.
[22] TURCHETTI G., ZANLUNGO F. and GIORGINI B., *EPL*, **78** (2007) 58003.
[23] XI J.-A., ZOU X.-L., CHEN Z. and HUANG J.-J., *Transp. Res. Procedia*, **2** (2014) 60.
[24] BRŠČIĆ D., KANDA T., IKEDA T. and MIYASHITA T., *IEEE Trans. Hum.-Mach. Syst.*, **43** (2013) 522.